J. Fluid Mech. (2002), *vol.* 453, *pp.* 153–175.
DOI: 10.1017/S0022112001006814 Printed in the United Kingdom

Long-wave instabilities of non-uniformly heated falling films

By SVETLA MILADINOVA[1], SLAVTCHO SLAVTCHEV[1], GEORGY LEBON[2] AND JEAN-CLAUDE LEGROS[3]

[1]Department of Fluid Mechanics, Institute of Mechanics, Sofia 1113, Bulgaria

[2]Institute of Physics, University of Liege, B 4000 Liege, Belgium

[3]Microgravity Research Center, Universite Libre de Bruxelles, B 1050 Brussels, Belgium

(Received 24 July 2000 and in revised form 18 July 2001)

We consider the problem of a thin liquid layer falling down an inclined plate that is subjected to non-uniform heating. The plate temperature is assumed to be linearly distributed and both directions of the temperature gradient with respect to the flow are investigated. The film flow is not only influenced by gravity and mean surface tension, but in addition by the thermocapillary force acting along the free surface. The coupling of thermocapillary instability and surface-wave instabilities is studied for two-dimensional disturbances. Applying the long-wave theory, a nonlinear evolution equation is derived. When the plate temperature is decreasing in the downstream direction, linear stability analysis exhibits a film stabilization, compared to a uniformly heated film. In contrast, for increasing temperature along the plate, the film becomes less stable. Numerical solution of the evolution equation indicates the existence of permanent finite-amplitude waves of different kinds. The shape of the waves depends mainly on the mean flow and the mean surface tension, but their amplitudes and phase speeds are influenced by thermocapillarity.

1. Introduction

Liquid films falling down an inclined heated plate occur in many experimental setups and technological applications. Such films are susceptible to long-wavelength instabilities. The interfacial waves propagating along the plate show fascinating nonlinear phenomena, such as solitary waves, transverse secondary instabilities, and complex disordered patterns. The problem of waves in falling films has been a subject of numerous experimental and theoretical studies (see the review papers by Chang 1994 and Oron, Davis & Bankoff 1997, as well as the book by Alekseenko, Nakoryakov & Pokusaev 1994 and the references therein). The earliest studies of isothermal films are based on linear stability analysis (Benjamin 1957; Yih 1963). These authors show that the vertical uniform film is always unstable. The instability of thin liquid films is manifested as gravity-driven surface waves with a wavelength much larger than the mean thickness of the film. The flat film on an inclined plate is unstable to long-wave disturbances for Reynolds numbers greater than $R_c = (5/2)\cot\beta$, where β is the angle of inclination with the horizontal. Applying the lubrication approximation to the Navier–Stokes equations, Benney (1996) derived a nonlinear evolution equation for two-dimensional flows. Such equations are much simpler than the full dynamic equations and are often used to study the nonlinear behaviour of film flows. A weakly nonlinear analysis based on Benney-type equations exhibits a bifurcation

of the solution giving rise to supercritical or subcritical instabilities of the waves (Gjevik 1970; Lin 1974). Supercritical finite-amplitude permanent waves exist for wavenumbers just below the critical wavenumber of the linear instability. A more complete nonlinear stability analysis for two-dimensional flows has been proposed by Pumir, Manneville & Pomeau (1983), confirming the results of the weakly nonlinear theory. They predict the existence of solitary waves for wavenumbers much smaller than the cut-off wavenumber. Numerical calculations based on the long-wave approximation provide limiting values of the Reynolds number, beyond which there are no stationary travelling waves and solutions of the evolution equation blow up for finite time.

The boundary layer approach is commonly used to study the nonlinear behaviour of falling films at high Reynolds number (Shkadov 1967; Demekhin & Shkadov 1985; Alekseenko, Nakoryakov & Pokusaev 1985; Trifonov & Tsvelodub 1991; Prokopiou, Cheng & Chang 1991; Chang, Demekhin & Kopelevich 1993). Salamon, Armstrong & Brown (1994) and Ramaswamy, Chippada & Joo (1996) studied two-dimensional surface wave instabilities by direct numerical simulation of the full nonlinear system of equations. They observe no tendency to wave breaking. They also confirm the results of the long-wave theory for small-amplitude waves. Recent experiments performed by Liu, Paul & Gollub (1993) and Liu, Schneider & Gollub (1995) exhibit a good agreement with the linear stability analysis on the value of the critical Reynolds number, growth rates and wave velocities.

Falling films on a heated plate are not only susceptible to surface wave instabilities but also to instabilities driven by shear stresses arising from the temperature dependence of the surface tension (the so-called Marangoni effect). The Marangoni effect in non-isothermal falling films was first examined by Lin (1975), Sreenivasan & Lin (1978), and later by Kelly, Davis & Goussis (1986) and Joo, Davis & Bankoff (1991). These authors consider a thin liquid layer flowing down an inclined, *uniformly* heated plate and examine the interaction of the two modes of instability. Applying the long-wavelength approximation, Kelly *et al.* (1986) examine the linear instability problem of films on weakly inclined plates. They establish that thermocapillarity has a destabilizing effect on the flow. Further, Goussis & Kelly (1990, 1991) extend their analysis and identify the surface-wave instability as well as two types of thermocapillary instability.

Treating the same problem, Joo *et al.* (1991) study the influence of evaporation on the long-wave instabilities. They apply the nonlinear stability theory and obtain similar results. In particular, they find that when the slope increases, the effect of the mean flow becomes more significant and the thermocapillary force amplifies the disturbances. The wave steeping and the surface fingering tend to develop at earlier times. It is also shown that when the thermocapillary effect is dominant, equilibration of the secondary flow is not observed. Spontaneous ruptures of the film surface are also predicted. However, in the relevant evolution equation, the terms depending on the Marangoni number are of second order in comparison with those due to gravity and mean flow.

The direct numerical simulations of the nonlinear non-isothermal problem of instability in a horizontal layer, made by Krishnamoorthy, Ramaswamy & Joo (1995), also show the occurrence of ruptures. For films of small thickness and at moderate heating, Joo, Davis & Bankoff (1996) analyse the nonlinear interaction between surface-wave and thermocapillary instabilities as well as the formation of longitudinal rolls. So far, there are not sufficient experimental results for a detailed comparison with the available theoretical results to be made.

Among the different physical situations mentioned above, thin falling films on a vertical or inclined *non-uniformly* heated plate, have not been examined theoretically. Thermocapillary instabilities have been studied in horizontal layers (Smith & Davis 1983; Davis 1987) where the imposed temperature gradient has a component parallel to the free surface so that fluid motion is generated by the tangential stresses, due to thermocapillarity. Smith & Davis (1983) determine neutral stability curves that exhibit a two-branch structure. One branch moves away from zero wavenumber for large values of the Marangoni number. This mode is a temperature disturbance that propagates in a direction depending on the magnitude of the Prandtl number. The second instability mode is of gravitational origin and is caused by the surface deformation.

Recently Kabov, Marchuk & Chupin (1996), Kabov (1998), Kabov *et al.* (1999) and Scheid *et al.* (2000) reported experiments on films falling down a vertical, locally heated wall. A constant heat flux was imposed on a rectangular area of the wall. In the last of these experiments the horizontal size of the rectangle is taken to be much larger than the vertical one, to ensure the presence of two-dimensional flows. Indeed, at small flow rates and heat fluxes, almost two-dimensional structures are observed in the middle region of the heated area. In particular, a stationary bump in the free surface appears close to the upper side of the rectangle. Such a strong surface deformation is due to the thermocapillary force acting along the interface in a direction opposed to the gravity force. Direct measurements of the surface temperature confirm this conclusion, because the temperature first increases significantly to reach a maximum and then decreases monotonically in the downstream direction. Above some critical value of the heat flux (depending on the flow rate), regular three-dimensional patterns are also observed. There exist several vertical 'horse-shoe'-like structures whose number depends on the magnitude of the heat flux through the wall. So far, there exists no theoretical model that describes these features of the film flow on a locally heated wall. It is worth noting that the distribution of the interface temperature can be represented locally by a linear function of the longitudinal coordinate, especially in the region below the bump where it decays monotonically.

The aim of the present study is to examine the nonlinear dynamic behaviour of a falling liquid film on an inclined plate with a temperature field that increases or decreases linearly in the downstream direction. The constant temperature gradient imposed along the plate affects the basic flat-film state as well as the surface-wave instabilities induced by gravity. We consider small flow rates and moderate temperature gradients for which the thermocapillary force is important and comparable to the gravity one. The linear stability analysis of a thin liquid layer on a non-uniformly heated plate recently performed by Kalitzova-Kurteva, Slavtchev & Kurtev (2000) in the case of infinitesimal wavenumbers, exhibits the role of Marangoni effect on the magnitude of the critical Reynolds number. Here we extend their study to the finite-amplitude long-wave instabilities of two-dimensional films. A nonlinear evolution equation is derived from the governing equations of mass, momentum and energy. It is solved analytically and numerically for reasonable values of the characteristic parameters.

The paper is organized as follows. In § 2, we present the physical model for the film flow and the heat transfer. In § 3, a linear stability analysis is developed and a numerical method for solving the basic evolution for the film thickness is briefly discussed. Numerical results describing the nonlinear effects are presented in § 4. In § 5, a linear stability analysis for three-dimensional disturbances is proposed and the main results are summarized.

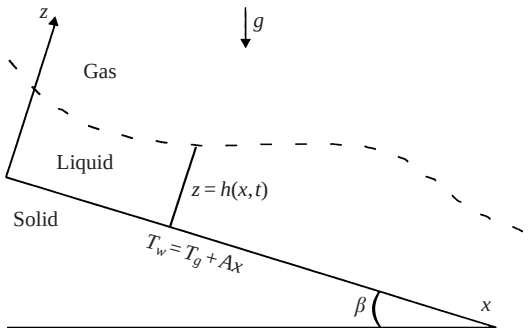

FIGURE 1. Sketch of an inclined falling film.

2. Formulation of the physical model

The physical system under consideration, shown in figure 1, consists of a thin liquid film which is draining down a rigid plate inclined at angle β with the horizontal. A constant temperature gradient A is imposed along the plate. Both positive and negative values of A are considered. The film is bounded above by a motionless gas at ambient temperature T_g and pressure p_g. The free surface is assumed adiabatic. The liquid is Newtonian with constant density ρ, kinematic viscosity ν and thermal diffusivity χ. The surface tension σ depends linearly on temperature T:

$$\sigma = \sigma_0 - \gamma(T - T_g), \tag{2.1}$$

where σ_0 is the mean surface tension at temperature T_g and $\gamma = -\mathrm{d}\sigma/\mathrm{d}T$ is a positive constant for most common liquids.

To formulate the two-dimensional hydrodynamic and thermal problem, Cartesian coordinates x, z are chosen with x as the streamwise coordinate and z being measured normal to the plate. The origin is located on the plate surface, where the temperature is equal to T_g. The wall temperature is given by

$$T_w = T_g + Ax \tag{2.2}$$

and increases (decreases) in the streamwise direction with positive (negative) A.

We assume that the liquid film is very thin, the heat flux weak, and the induced gravity-driven flow is relatively slow, so that the flow regime is close to that predicted by the lubrication theory. It means that the velocity and temperature vary slowly along the plate and the length of the surface waves is much larger than the mean film thickness (denoted by d_0).

The dynamical behaviour and heat transfer in the film are determined by four time scales: the viscous time $t_{visc} = d_0^2/\nu$, the gravitational time $t_{grav} = (d_0/g)^{1/2}$, the mean surface tension time $t_{surf} = (\rho d_0^2/\sigma_0)^{1/2}$, and the thermal diffusion time $t_{therm} = d_0^2/\chi$, where g is the gravitational acceleration. These characteristic times are not all of the same order. For very thin films the main characteristic time is the viscous one. The thermal diffusion time is given by $t_{therm} \approx t_{visc}$ for liquids with the Prandtl number $P = \nu/\chi = O(1)$. We also assume that $t_{grav} \approx t_{visc}$, which means that the Galileo number $G \equiv t_{visc}^2/t_{grav}^2 = g d_0^3/\nu^2$ representing the ratio of the gravity force ρg to the viscous force $\mu\nu/d_0^3$, is of order of unity (μ is the dynamic viscosity). The characteristic time related to the mean surface tension is usually much smaller than the viscous time and the surface parameter $S_M \equiv t_{visc}^2/t_{surf}^2 = \sigma_0 d_0/\rho\nu^2$, representing for the ratio of the capillary force, σ_0/d_0, to the viscous one, is quite large.

In thin films the coordinate z and the interface position, $z = h(x,t)$, are scaled by the mean thickness of the film, while the longitudinal coordinate x is measured by a length, l, proportional to the disturbance wavelength. As we consider long-wavelength instabilities, the quantity l is much larger than d_0, i.e. the ratio $\varepsilon \equiv d_0/l$ is a small parameter. We choose the scales ld_0/ν, ν/d_0, ν/l and $\rho\nu^2/d_0^2$, for the time, t, the streamwise velocity, u, the transverse velocity w, and the pressure difference, $p - p_g$, respectively. The same scales are used for isothermal thin falling films as well as non-isothermal ones on a uniformly heated wall. In contrast to previous studies, the temperature difference $T - T_g$ is here scaled by the quantity Al which measures the temperature difference along the plate between two points distant from each other by a wavelength.

The governing equations are the equations of continuity, momentum and energy written in dimensionless form:

$$u_x + w_z = 0, \tag{2.3}$$

$$\varepsilon[u_t + uu_x + wu_z] = -\varepsilon p_x + \varepsilon^2 u_{xx} + u_{zz} + R, \tag{2.4}$$

$$\varepsilon^2[w_t + uw_x + ww_z] = -p_z + \varepsilon^2 w_{xx} + \varepsilon w_{zz} - R\cot\beta, \tag{2.5}$$

$$\varepsilon P[\theta_t + u\theta_x + w\,\theta_z] = \varepsilon^2\theta_{xx} + \theta_{zz}, \tag{2.6}$$

where the notation for the dimensional and dimensionless variables is kept the same, except that the dimensionless temperature is denoted by θ, $R = G\sin\beta$ is taken as the Reynolds number. The subscripts denote differentiation with respect to the indicated variable. The variation of the density with temperature is negligible in very thin layers.

The corresponding boundary conditions are the following. At the rigid plate ($z = 0$)

$$u = w = 0, \tag{2.7}$$

with a temperature distribution given by

$$\theta = x. \tag{2.8}$$

The normal and tangential stress balances at the interface, $z = h(x,t)$, are written as

$$p + 2\varepsilon\frac{(1-\varepsilon^2 h_x^2)}{(1+\varepsilon^2 h_x^2)}u_x + \frac{2\varepsilon h_x}{(1+\varepsilon^2 h_x^2)}(u_z + \varepsilon^2 w_x) = -\varepsilon^2 S_M\frac{(1 - Ca\theta)\,h_{xx}}{(1+\varepsilon^2 h_x^2)^{3/2}}, \tag{2.9}$$

$$\frac{(1-\varepsilon^2 h_x^2)}{(1+\varepsilon^2 h_x^2)^{1/2}}(u_z + \varepsilon^2 w_x) - \frac{4\varepsilon^2 h_x}{(1+\varepsilon^2 h_x^2)^{1/2}}u_x = -\frac{\varepsilon Ma}{P}(\theta_x + h_x\theta_z). \tag{2.10}$$

The last boundary condition for the velocity at the interface is the kinematic condition

$$w = h_t + uh_x. \tag{2.11}$$

The free surface is considered to be thermally insulated, i.e.

$$-\varepsilon^2 h_x\theta_x + \theta_z = 0. \tag{2.12}$$

The non-dimensional parameters appearing in (2.9) and (2.10) are the Marangoni and capillary numbers defined respectively by

$$Ma = \frac{\gamma Ald_0}{\mu\chi}, \quad Ca = \frac{\gamma Al}{\sigma_0}. \tag{2.13}$$

The Marangoni and capillary numbers take positive or negative values depending on the direction of the temperature gradient. According to the experiments of Kabov

(1998) on films of aqueous solutions of ethyl alcohol, we estimate that $|Ma| = O(\varepsilon^{-1})$, $S_M = O(\varepsilon^{-2})$ and $|Ca| = O(\varepsilon)$ for a mean thickness $d_0 = 10^{-4}$ m and $|A| = 1\,\mathrm{K\,cm^{-1}}$. Let us also introduce the new parameters $Mn = \varepsilon Ma/P$ and $S = \varepsilon^2 S_M$, which are of the order of unity, and substitute them into (2.9) and (2.10). At the zero approximation with respect to ε, the thermocapillary force represented by the right-hand side of (2.10) is comparable with the viscous stresses. Moreover, for $R \sim O(1)$, $P \sim O(1)$, $S \sim O(1)$ and $|Mn| \sim O(1)$, the gravity, viscous, capillary and thermocapillary forces are of the same order and their effect occurs simultaneously at the zero-order approximation.

3. Long-wave approximation

3.1. *Nonlinear evolution equation*

The solution of the problem is obtained by expanding the variables in power series in ε, namely

$$u = u^0 + \varepsilon u^1 + \ldots, \quad w = w^0 + \varepsilon w^1 + \ldots, \quad p = p^0 + \varepsilon p^1 + \ldots, \quad \theta = \theta^0 + \varepsilon \theta^1 + \ldots. \tag{3.1}$$

The film thickness $h(x,t)$ and its derivatives are assumed to be of order of unity. Following Benney's approach (Benney 1966), the complicated nonlinear system (2.3)–(2.12) can be reduced to a single nonlinear evolution equation for the film thickness. We proceed with the asymptotic analysis by substituting expressions (3.1) into the set (2.3)–(2.12). After equating to zero the coefficients of the same powers of ε in each equation and boundary condition, we obtain a sequence of equations. We first determine the velocity components as functions of the unknown film thickness. The solutions are then substituted into the kinematic condition (2.11) and the resulting equation describes the evolution of the interface.

At the zeroth-order approximation, the set of equations and boundary equations is

$$u^0_{zz} = -R, \quad p^0_z = -R\cot\beta, \quad u^0_x + w^0_z = 0, \quad \theta^0_{zz} = 0, \tag{3.2}$$

$$z = 0: \quad u^0 = w^0 = 0, \quad \theta^0 = x, \tag{3.3}$$

$$z = h(x,t): u^0_z = -Mn\left(\theta^0_x + h_x\theta^0_z\right), \quad p^0 = -Sh_{xx}, \quad \theta^0_z = 0. \tag{3.4}$$

The solution of this system is

$$u^0 = -R\frac{z^2}{2} + (Rh - Mn)z, \quad w^0 = -Rh_x\frac{z^2}{2}, \tag{3.5}$$

$$p^0 = R\cot\beta(h - z) - Sh_{xx}, \tag{3.6}$$

$$\theta^0 = x. \tag{3.7}$$

Note that the thermocapillarity influences the longitudinal velocity even at the zeroth-order approximation. The surface velocity, expressed by

$$u^S = R\frac{h^2}{2} - Mn\,h, \tag{3.8}$$

differs from that for isothermal films, becoming smaller with increasing temperature ($Mn > 0$) and respectively larger with decreasing temperature along the plate ($Mn < 0$).

At the first-order approximation,

$$u^1_{zz} = p^0_x + u^0_t + u^0 u^0_x + w^0 u^0_z, \tag{3.9}$$

$$w^1 = -\int_0^z u^1_x \mathrm{d}y, \quad p^1_z = w^0_{zz} = -Rh_x, \tag{3.10}$$

$$\theta^1_{zz} = P\ u^0, \tag{3.11}$$

$$z = 0 : u^1 = w^1 = 0, \quad \theta^1 = 0, \tag{3.12}$$

$$z = h(x,t) : u^1_z = -Mn(\theta^1_x + h_x\theta^1_z), \quad p^1 = -2(u^0_x + h_x u^0_z), \quad \theta^1_z = 0. \tag{3.13}$$

After integration, the functions θ^1, u^1 and w^1 are expressed in analytical form (not presented here). Substituting u^0, u^1, w^0 and w^1 into (2.11), one obtains the equation for the thickness h in the case of two-dimensional nonlinear waves, namely

$$h_t + (Rh - Mn)hh_x + \varepsilon\left[\tfrac{1}{3}h^3(Sh_{xxx} - R\cot\beta\, h_x) + \tfrac{2}{15}Rh^5h_x(Rh - Mn)\right]_x + \varepsilon\left[\tfrac{1}{2}PMnh^4h_x\left(\tfrac{5}{6}Rh - Mn\right)\right]_x + O(\varepsilon^2) = 0. \tag{3.14}$$

This equation is similar to that derived by Joo *et al.* (1991) for uniformly heated inclined plate (without evaporation), but contains additional terms, due to the non-uniformity of the plate temperature.

In what follows the evolution equation (3.14) will be solved by applying both a linear and a weakly nonlinear stability analysis.

3.2. *Linear analysis*

The basic state is represented by (3.5)–(3.7) with $h = 1$. For a parallel shear flow, equation (3.14) admits normal-mode solutions of the form

$$h(x,t) = 1 + \delta_0 \exp(\mathrm{i}kx - \omega_0 t), \tag{3.15}$$

where the amplitude $\delta_0 \ll 1$, k is the scaled streamwise wavenumber, and $\omega_0 = \omega_R + \mathrm{i}\omega_I$ is the frequency. For temporal stability analysis, k is real and ω_0 is a complex number. By substituting the above expression into (3.14) and linearizing with respect to δ_0, the linear growth rate of the perturbation is obtained. When the thermocapillary force is comparable with the viscous and gravity forces, the linearized phase speed is given by

$$c_0 = \frac{\omega_I}{k} = R - Mn \tag{3.16}$$

and the growth rate by

$$\omega_R = \varepsilon k^2\left[\tfrac{2}{15}R^2 - \tfrac{1}{3}R\cot\beta - \tfrac{1}{3}k^2S + \tfrac{5}{12}\left(P - \tfrac{8}{25}\right)RMn - \tfrac{1}{2}PMn^2\right]. \tag{3.17}$$

Thermocapillarity influences both physical parameters. The phase speed decreases (increases) when the plate temperature increases (decreases) in the downstream direction. This result differs from Joo *et al.* (1991) stating that in uniformly heated layers the linearized phase speed remains unaffected by the thermocapillary force.

The condition for linear instability of a uniform film is $\omega_R > 0$. The first term in (30) expresses the destabilizing effect of the mean flow while the second and third ones exhibit stabilizing effects of the hydrostatic pressure and mean surface tension. For liquids with $P \geqslant 1$ considered here, the sign of the fourth term in (3.17) coincides with that of the Marangoni number. Therefore, thermocapillarity is stabilizing when the plate temperature is decreased ($Mn < 0$) and destabilizing for temperature increasing

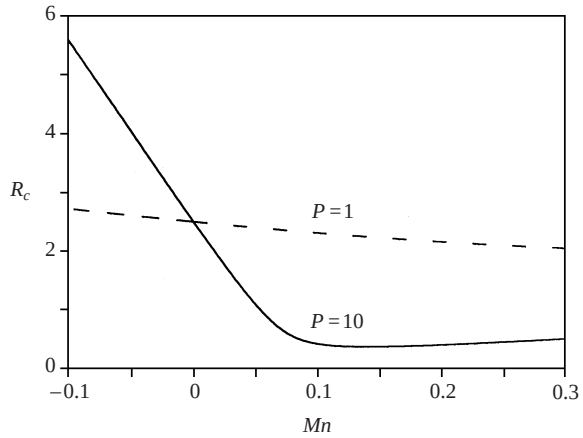

FIGURE 2. Marginal stability Reynolds number as function of Mn for $\beta = \pi/4$, $S = 0$ and values of the Prandtl number: $P = 1$ (dashed line) and $P = 10$ (solid line).

in the downstream direction ($Mn > 0$). The sign of the fifth term in (3.17) is negative whatever the sign of Mn, so that it has always a stabilizing effect that might be less important than the effect of the fourth term.

The influence of gravity and thermocapillarity on the film instability is shown in figure 2, displaying the critical Reynolds number versus Mn for $S = 0$ for two values of the Prandtl number (a dashed line for $P = 1$ and a solid one for $P = 10$). For inclined layers ($\beta \neq \pi/2$ and $R \neq 0$), there exists a stable region below each curve, due to the hydrostatic pressure and thermocapillarity. The Marangoni number, for which the critical Reynolds number is the smallest, depends strongly upon the Prandtl number P. Also, the influence of P on the two-dimensional stability threshold is related to the sign of the temperature gradient: when Mn is negative, R_c increases with P while for positive values of Mn it decreases with increasing P.

In summary, the linear decrease in plate temperature is always a stabilizing factor for infinitesimal perturbations. Increasing the plate temperature has a destabilizing effect at some Prandtl numbers. But, for relatively large Prandtl numbers, large temperature gradients can stabilize the flow. A similar non-monotonic influence of the heating along the rigid wall on the film instability was found by López, Bankoff & Miksis (1996) for a non-isothermal film moving down an inclined plate in the presence of contact line.

When the capillary force at the free surface is taken into account, there exists a cut-off wavenumber, k_c, for which the linear growth rate vanishes. The growth rate has a maximum for $k_m = k_c/\sqrt{2}$. In figure 3, the cut-off wavenumber is plotted against the Reynolds number for $\beta = \pi/4$, $S = 0.3$ and $P = 10$. The bifurcation points R_c, the upper neutral curve $k = k_c$ and the lower neutral curve $k = 0$ are represented for several values of Mn. The flow is linearly unstable when $R > R_c$ and $0 < k < k_c$. It is seen that the neutral curves move from left to right as Mn varies from positive to negative values. Moreover, for a given R, the cut-off wavenumber decreases with the Marangoni number. Calculations for different values of the surface parameter show that the increase of S leads to an extension of the band of stable wavenumbers. In short, the linear stability analysis shows that an increase in plate temperature destabilizes the film while a temperature decrease has a stabilizing effect compared to a uniformly heated film.

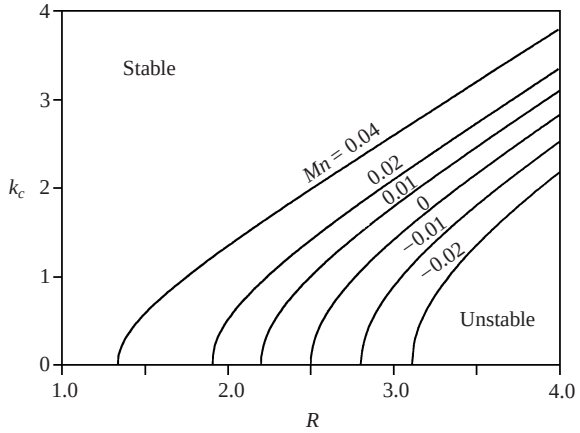

FIGURE 3. Marginal stability wavenumber as function of the Reynolds number for $\beta = \pi/4$, $P = 10$, $S = 0.3$ and different values of the Marangoni number.

3.3. *Nonlinear analysis*

In this subsection, we will study the evolution of finite-amplitude perturbations to better understand the mechanism responsible for the transfer of energy from the basic state to the disturbance. The initial disturbance is taken to be a monochromatic wave with small amplitude

$$h(x, 0) = 1 - \delta_1 \cos(kx). \tag{3.18}$$

The amplitude δ_1 will be taken constant and equal to 0.1, as Joo & Davis (1992) demonstrated that the final state of the disturbance is not sensitive to it. At the initial time, the waves differ by their wavenumbers. The time evolution of the waves is obtained by solving equation (3.14) by means of the finite difference method. The equation is written in a conservative form and integrated in a periodic domain. A second-order-accurate Crank–Nicholson scheme is used in time and a modified second-order upwind difference method is employed to handle the nonlinear terms. The method possesses both conservative and transport properties and maintains approximately the second-order accuracy of centred-space derivatives. The nonlinear difference equations are solved by Newton–Ralphson iteration.

The initial value problem is solved in the interval $[-\pi/k, \pi/k]$. The mesh spacing, $\Delta x = 10^{-3}$, and the time step, varying from 5×10^{-5} to 5×10^{-4}, are small enough to obtain a solution with satisfactory accuracy. The accuracy is controlled by checking the averaged thickness

$$\bar{h} = \frac{k}{2\pi} \int_{-\pi/k}^{\pi/k} h(x, t)\, \mathrm{d}x,$$

which is constant in time, as follows directly from (3.14). For the initial profile (3.18), $\bar{h} = 1$. If Δx and Δt are chosen too large, the numerical value of $\bar{h}$ drifts monotonically away from 1 as time elapses. Smaller time steps than the maximum one, $\Delta t = 5 \times 10^{-4}$, are selected when the wave amplitude begins to grow explosively. We choose physically reasonable values of the non-dimensional parameters. To compare our numerical results with those obtained by Joo *et al.* (1991), we take $\varepsilon = 0.2$ and $S = 0.3$.

4. Results

4.1. *Isothermal layers*

The numerical method is first implemented for isothermal films. We confirm the results of the nonlinear theory reported in previous studies (e.g. Joo *et al.* 1991), extending them to larger values of the mean surface parameter and smaller wavenumbers.

The weakly nonlinear analysis predicts that the evolution of the two-dimensional waves depends strongly on the initial wavenumber (Gjevik 1970; Lin 1974; Chang 1989). This conclusion is also confirmed by numerical simulations based on the Benney-type long-wave approximations (Joo *et al.* 1991). Let us summarize the main results of the linear and weakly nonlinear theory for isothermal films.

(i) For $k > k_c$, the initial perturbation of the flat film surface is damped and the wave damping process becomes slower as $k \to k_c$. At large times, the solution tends to the basic state, $h = 1$.

(ii) The weakly nonlinear analysis predicts the occurrence of another wavenumber $k_s(R, \beta, S)$, which separates the regimes of supercritical ($k_s < k < k_c$) and subcritical ($k < k_s$) domains. In the regime of supercritical bifurcations, the initial perturbation grows and changes its shape. After some time the flow equilibrates, but the convergence towards the equilibrium state is not monotonic. For a wavenumber k close to k_c, the solution may evolve into a stable, almost sinusoidal wave of small finite amplitude. For k close to k_m, the surface wave approaches the form of a 'solitary' (or single) wave, as observed in experiments. Gjevik (1970) found that $k_s = k_c/2$, and the theoretical approaches of Lin (1969, 1974) and Chang (1989) predict similar results. However, in their numerical calculations Joo *et al.* (1991) did not reach equilibration at $k = k_c/2$, but demonstrated that the value of k_s would necessarily be larger than $k_c/2$. Pumir *et al.* (1983) noted that several kinds of degenerate solitary waves may exist.

(iii) When $k < k_s$, a strong nonlinearity promotes further change in the initial disturbance and saturation does not occur. However, the weakly nonlinear analysis cannot predict properly the wave evolution in the regime of subcritical instability. Some previous attempts to solve the long-wave evolution equation for k much smaller than k_c have also failed, due to numerical breakdown (Pumir *et al.* 1983 and Joo *et al.* 1991).

In the present paper, we study the nonlinear long-wave instability in isothermal films ($Mn = 0$) for initial wavenumbers smaller than the cut-off one. For Reynolds number $R = 3.53$ and $\beta = \pi/4$, the linear theory predicts $R_c = 2.5$, $k_c = 2.21$ and $k_m = 1.56$. In figures 4 and 5, some stability results are presented for the wavenumbers $k = 1.3$ and 0.7, respectively. In figure 4(*a*,*b*), free-surface configurations are shown by lines representing a time increment of 0.05. For small times, the wave amplitude first grows, in accordance with the linear theory, but soon reaches a maximum and then decays slowly. It is seen from figure 4(*c*) that a finite-amplitude permanent wave emerges after about 20 nondimensional time units and travels downstream with a fixed wave speed. In the same figure, the final permanent waveform predicted by Joo *et al.* (1991) is represented by a dashed line. There is a good agreement between our results and these obtained by different numerical methods, even though the permanent waves occur at different periods of time.

Figure 5 shows the surface-wave instability for $k = 0.7$, which is less than one-third of k_c. It is found that the growth rate is much more important and the distortion of the free surface is more significant for smaller initial wavenumbers. The initial sinusoidal shape is distorted, so that the wave front steepens and its rear is stretched (figure 5*a*). The wave amplitude decays after reaching a maximum and the wave

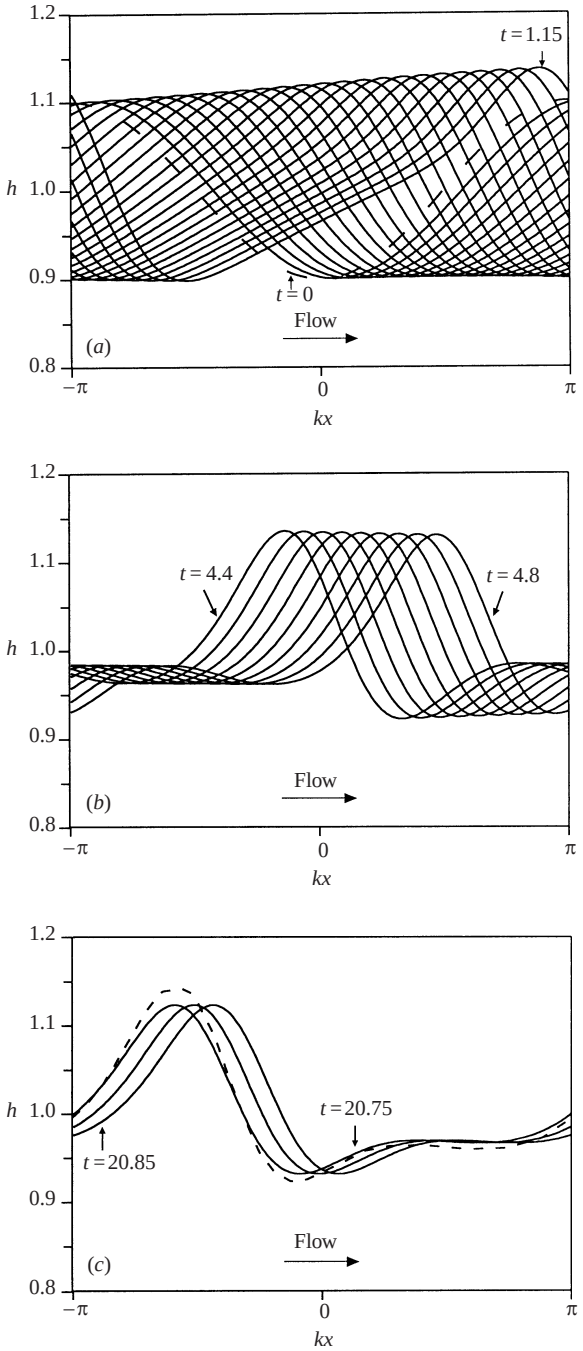

FIGURE 4. Evolution of the free-surface shape of an isothermal layer at various instants of time for $R = 3.53$ and $k = 1.3$ ($k_m = 1.56$): (*a*) from $t = 0$ to $t = 1.15$ in steps of 0.05; (*b*) from $t = 4.4$ to $t = 4.8$ in steps of 0.05; (*c*) final permanent waveforms for $20.75 \leqslant t \leqslant 20.85$ with time increment of 0.05. The permanent wave calculated by Joo *et al.* (1991) for $t = 29.85$ is represented by the dashed line.

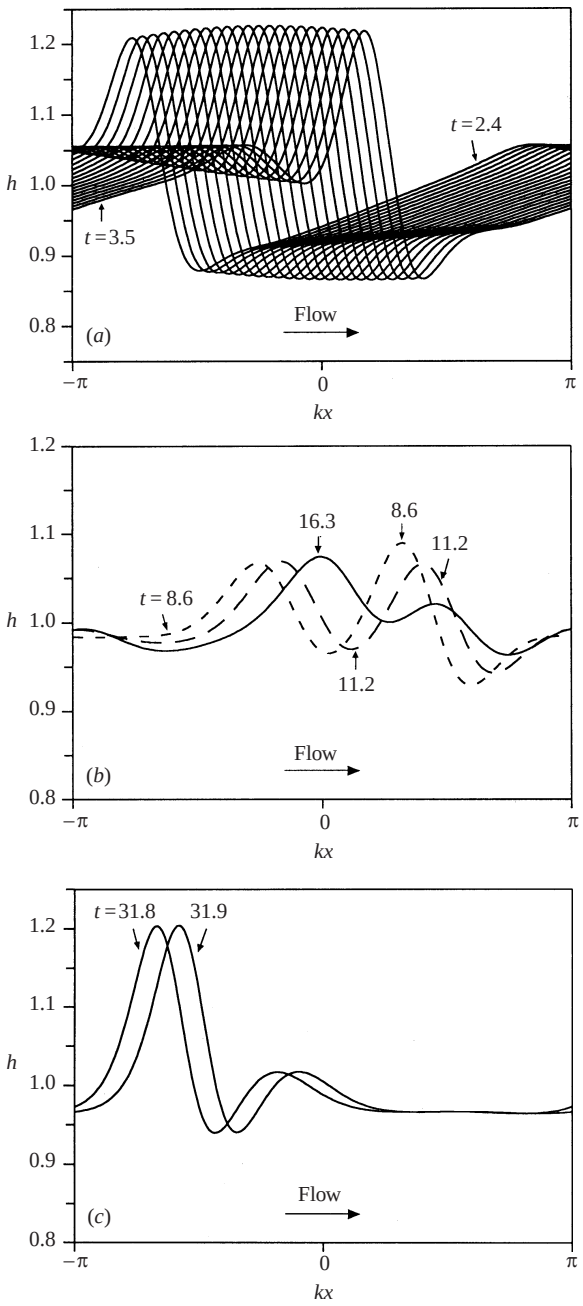

FIGURE 5. Evolution of the free-surface shape of an isothermal layer at various instants of time for $R = 3.53$ and $k = 0.7$. (*a*) from $t = 2.4$ to $t = 3.5$ in steps of 0.05; (*b*) film profiles: - - -, $t = 8.6$; ——, $t = 11.2$; —, $t = 16.3$; (*c*) final permanent waveforms at $t = 31.8$ and $t = 31.9$.

rear becomes longer and longer with the appearance of dimples. The large-amplitude wave is then followed by a small-amplitude capillary wave.

Pumir *et al.* (1983), Joo *et al.* (1991), and Joo & Davis (1992) reported an explosive wave growth occurring at rather small initial wavenumbers. For a finite period of

time the perturbations will grow, reaching a large amplitude, then start to evolve quickly but after some time the numerical calculations break down. For $k = 0.7$ (i.e. $k < k_c/2$), our numerical procedure allows us to follow the solution over long periods of time and to observe new features. Over such times, the large-amplitude wave travels faster and disperses into capillary ripples of almost the same amplitudes, as seen in figure 5(*b*). There is a coalescence between the small-amplitude waves. The wave interaction continues for a long time, until only one 'solitary' wave is emerging (figure 5*c*). So, it appears that for quite small wavenumbers the preferred surface shape is a 'solitary' wave and such a behaviour is confirmed by experiments (Liu *et al.* 1993, 1995). A qualitative comparison of our results with the full-scale computations by Ramaswamy *et al.* (1996) indicates the capability of the long-wave approximation theory to predict the behaviour of the film thickness in the range of parameters for which it is developed. However, for relatively large values of the Reynolds number, the long-wave evolution equation does not give correct results as the large-amplitude disturbances require considering higher-order terms in the asymptotic presentation of the film thickness.

4.2. *Effect of thermocapillarity*

We examine now the evolution of a falling film on a plate with a temperature field decreasing or increasing linearly along the surface. It is well known that the long waves originate from the deformation of the free surface, due to the gravity and mean surface tension. The change of the film thickness and the imposed temperature gradient along the plate cause variations in the film surface temperature. Due to thermocapillarity, the liquid moves from warm depressed regions (troughs) of the film to the neighbouring cooled elevated regions (crests). The hydrostatic pressure tends to flatten the interface and therefore stabilizes the surface perturbations. The instability of thin falling films being convective, the disturbances are transported downstream by the mean flow.

In this work, we consider an adiabatic free surface. This assumption is reasonable because the growing initial waves cause variations in the surface temperature, even in the case of a constant plate temperature. As shown below, the thermocapillary mechanism of instability is more significant for a linear distribution of the plate temperature than for a constant temperature. When studying the thermocapillary effect on the surface wave instability, two questions need to be answered: How is the nonlinear evolution of periodic waves affected by the linear distribution of the plate temperature? What kinds of permanent wave shapes are formed?

To answer these questions, the evolution equation (3.14) will be solved in two different ways. First, the solution will be found analytically, using the weakly nonlinear theory. Second, for strong nonlinear regime, the equation will be solved numerically in a periodic domain, using the finite-difference code described in § 3.3. It is natural to assume that the fluid domain is not restricted by periodicity and that the surface waves evolve both spatially and temporally, allowing complex wave interactions. However, from the mathematical point of view, it is not obvious how to formulate the boundary conditions on the free surface when leaving the domain under study. It is also unclear whether the limitation of the computational domain to a finite length may lead to artificially high critical values of R and Mn. Therefore we impose periodic boundary conditions, which simplifies greatly the numerical calculations and leads to physically reasonable results.

Applying the weakly nonlinear analysis to non-isothermal films, we prove the existence of the supercritical stability region, $k_c > k > k_s = k_c/2$, for relatively large

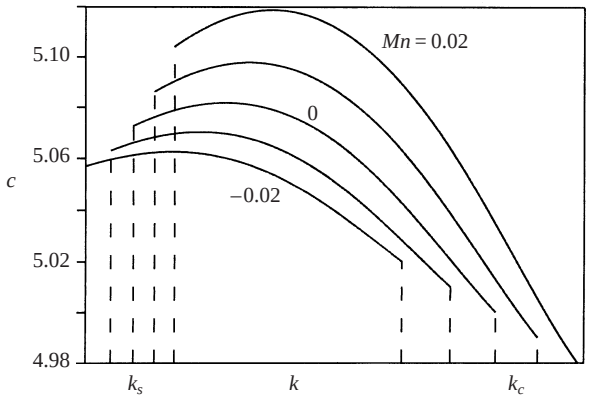

FIGURE 6. Nonlinear phase speed versus k for $R = 3.53$, $\beta = \pi/4$, $P = 10$, $S = 3$ and different values of Mn from -0.02 to 0.02 in steps of 0.01.

values of the mean surface parameter (when $S > 1$), as Gjevik (1970) reported previously for isothermal films. In this region, equilibration of the waves occurs as a result of saturation of dominant Fourier series terms. However, as k becomes closer to k_s, higher harmonics than those taken into account in the weakly nonlinear theory become important and the equilibration, if it exists, cannot be described by taking into account only the fundamental mode and a few subharmonics.

In figure 6, the wave speed c is plotted versus the wavenumber for $R = 3.53$, $\beta = \pi/4$, $P = 10$, $S = 3$ and different values of the Marangoni number. The nonlinear phase speed is always larger than the linearized one (see (3.16)). It increases with Mn at a given wavenumber. When k is decreased from the cut-off wavenumber, the wave speed increases and passes through a maximum. The rate of increase of c is smaller for negative Mn than for positive Mn. The wavenumber at which the speed has maximum is influenced by thermocapillarity and increases with the Marangoni number. The calculations show that the wave amplitude grows as Mn is increased.

The nonlinear evolution of the film is studied by solving equation (3.14) numerically. In this paper, numerical results are obtained for the inclination angle $\beta = \pi/4$, the Prandtl number $P = 10$ and the surface parameter $S = 0.3$.

4.2.1. *Linear decrease in plate temperature*

Consider first the case of a linear decrease in plate temperature in the downstream direction. Typical results of the numerical solution for negative Marangoni numbers are shown in figures 7 and 8. They display permanent waveforms for $R = 3.53$ and different initial wavenumbers. In figure 7, free-surface configurations are presented for $k = 1.3$ and two values of the Marangoni number: $Mn = -0.01$ (solid lines) and $Mn = -0.02$ (dashed line). For these values of Mn the film flow is linearly unstable as k_c is equal to 1.83 ($k_m = 1.3$) and 1.43 ($k_m = 1$). Up to moderate times ($t = 5.6$) the nonlinear wave evolution is similar to the isothermal case (compare with figure 4*b*), but the subsequent monotonic decay of the wave amplitude differs from that case. Due to thermocapillarity, the amplitude growth stops earlier than in the isothermal case and, for example, the permanent wave amplitude at $t = 13.8$ is lower than that for $t = 20.85$ in figure 4(*c*). For $Mn = -0.02$, the perturbation damps slowly and the free surface tends to the basic flat film.

Figure 8 displays permanent waves for $k = k_s(Mn)$. Note that $k_s = 1.1$ in the isothermal case (solid line) and $k_s = 0.7$ at $Mn = -0.02$ (dashed line). For $Mn = 0$,

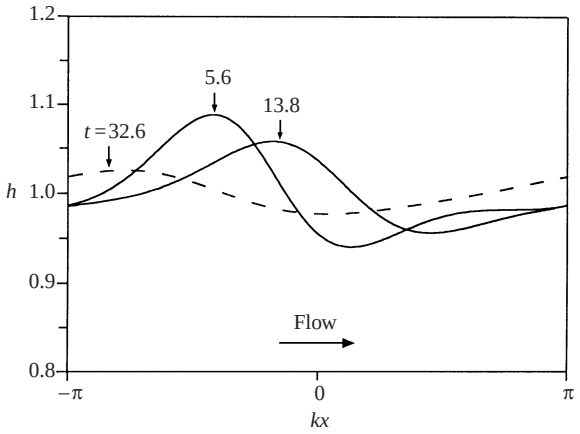

FIGURE 7. Free-surface configurations for a linear decrease in plate temperature for $R = 3.53$, $k = 1.3$ and two Marangoni numbers at different times: - - - , $Mn = -0.02$ at $t = 32.6$; —, $Mn = -0.01$ at $t = 5.6$ and $t = 13.8$ (final permanent waveform).

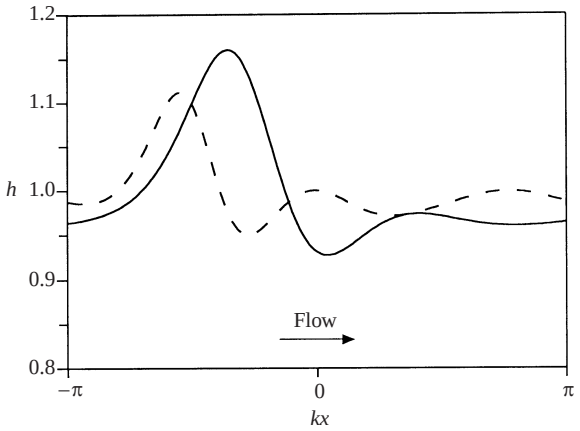

FIGURE 8. Final permanent waveforms for $R = 3.53$, $k = k_s(Mn)$ and two values of the Marangoni number: $Mn = 0$ (solid line) and $Mn = -0.02$ (dashed line).

the resultant wave grows initially in amplitude and travels downstream leaving behind it a nearly undeformed interface. This behaviour is similar to that shown in figure 5(a). Since the imposed wavenumber is half of the cut-off value, the most likely surface shape is expected to be a 'solitary' wave, and this is what is obtained. For $Mn = -0.02$, the disturbance amplitude grows slightly from its initial value and afterwards monotonically decays towards an equilibration form. A comparison between the permanent waves in figure 8 indicates that the decrease in plate temperature has a strong stabilizing effect on the film by restricting the growth of the wave amplitude. For $Mn = -0.02$ the finite-amplitude permanent wave travels downstream with a fixed speed smaller than the wave speed at $Mn = 0$.

The physical mechanism for the stabilizing effect of thermocapillarity when $Mn < 0$ can be explained in the following way. When the plate is cooled in the downstream direction (see the scheme in figure 9a) the surface temperature at the trough (point L) ahead of the moving wave front is lower than that at the crest (point M) and the thermocapillary force acting in the same direction tends to flatten the film. The

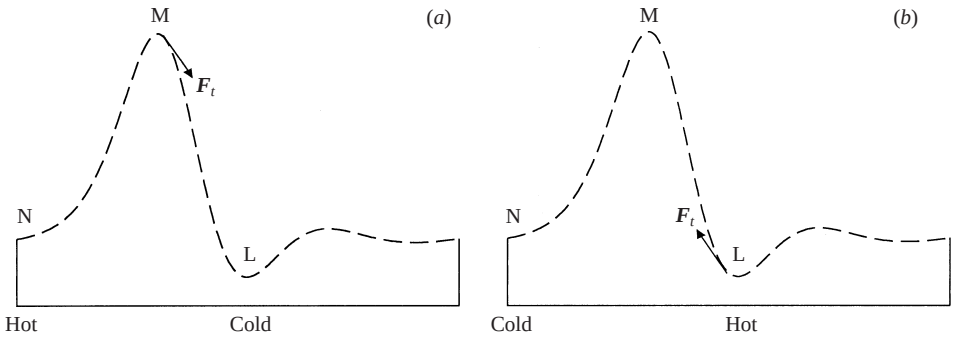

FIGURE 9. Scheme of the action of the thermocapillary force $\boldsymbol{F}_t$: (*a*) case of linear decrease in plate temperature, (*b*) case of linear increase in plate temperature.

depressed region behind the wave front (point N) is warmer than the elevated one (point M), but the calculations show that the tangential temperature gradients in the wave trailing region are quite small. Brauner & Maron (1982) studying the development of waves and their influence on mass transfer in a fluid layer flowing down an inclined plate, found that the major increase in the mass transfer rate occurs in the wave front region, while a decay in the transfer rate takes place in the trailing region. This observation seems to be a good but indirect confirmation of the present prediction about weak tangential temperature gradients in the trailing region. In summary, when the plate temperature is decreased in the downstream direction, thermocapillarity has a strong stabilizing effect on the surface wave evolution.

4.2.2. *Linear increase in plate temperature*

Suppose now that the temperature is increased linearly along the plate. In this case (see figure 9*b*), the thermocapillary force will draw the liquid from a hot trough (point L) to a cold crest (point M) in the direction opposite to gravity. The crest is then moving faster than the trough and the wave becomes steeper behind the trough. Therefore, when the depressed wave region tends to flatten and the crest to elevate, the tangential temperature gradient ahead of the wave front becomes larger and larger and the disturbance is amplified. The temperature differences in the wave trailing region (from M to N) are again small and the thermocapillary force acting along that portion of the surface is much weaker and does not influence significantly the film shape. Therefore, the destabilizing effect of the thermocapillary force acting ahead of the wave front will be dominant, as we will see below.

We start the calculations with the values of the Reynolds and Marangoni numbers and wavenumbers obtained from the linear stability analysis shown in figure 3. For such points as, for example, $Mn = 0.01$, $k = 1.5$ and $R = 1.7$ ($R_c = 2.8$), the initial perturbation damps quickly towards the basic state, as expected.

The evolution of the film thickness for values of R, Ma and k outside the stability region is displayed in figures 10–12. Free-surface configurations are shown in figure 10 for $R = 3.53$, $Mn = 0.02$ and $k = 1.3$. For these values of the Marangoni and Reynolds numbers it is found that $R_c = 1.9$, $k_c = 2.8$ and $k_m = 1.97$. At the initial stage, the amplitude of the disturbance grows quickly and the phase velocity in the crest becomes higher than in the trough. The wave deforms, having an asymmetric shape with a steep front (figure 10*a*). Due to thermocapillarity, the growth of the disturbance is amplified (figure 10*b*) and no equilibration is achieved, at least within the range of validity of equation (3.14). In the case of a non-adiabatic (evaporative) interface, a

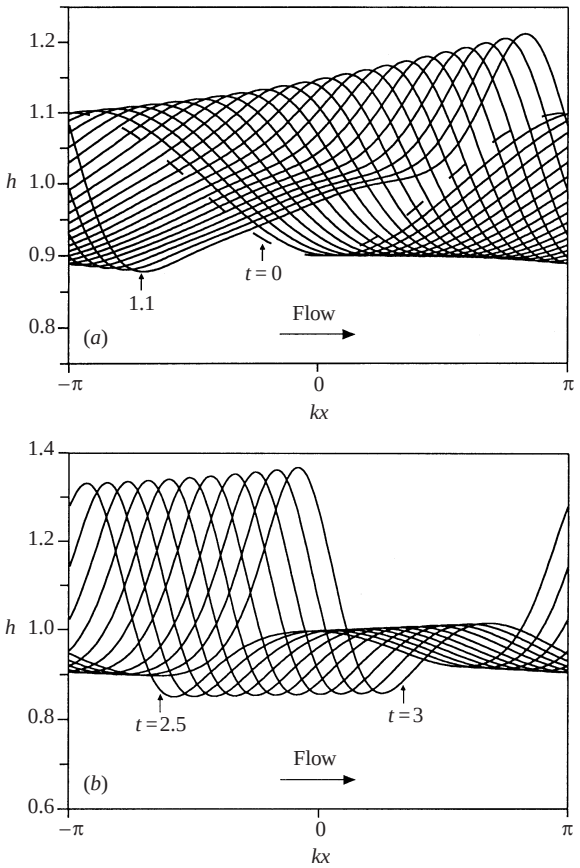

FIGURE 10. Free-surface configurations in the case of a linear increase in plate temperature for $R = 3.53$, $k = 1.3$ and $Mn = 0.02$ at various instants of time: (*a*) from $t = 0$ to $t = 1.1$ in steps of 0.05; (*b*) from $t = 2.5$ to $t = 3$ in steps of 0.05.

similar behaviour is predicted by Joo *et al.* (1991). Their surface configurations are similar to a monochromatic wave, but nevertheless an unbounded growth in the wave amplitude is found.

Figure 11(*a*) shows the film shapes for a smaller Reynolds number $R = 2.8$ and the same values of the other parameters as in figure 10. In this case the linear stability theory predicts $k_c = 1.83$ and $k_m = 1.3$. The values of the Reynolds number and the initial wavenumber corresponds to the point (2.8, 1.3) in figure 3, situated between the neutral curves $Mn = 0$ and $Mn = 0.02$, which means that while the relative isothermal film is linearly stable, the non-isothermal one is unstable. At the initial stage, the resultant wave grows in amplitude and travels downstream followed by a capillary ripple (similar shapes are displayed in figure 4*b*). It turns out that the disturbance tends toward a permanent wave, shown in figure 11(*a*). So, for k being equal to the wavenumber k_m corresponding to the maximum amplitude growth, an almost sinusoidal wave is observed at large times. This is a consequence of the balance between the gravity and thermocapillary forces.

When for the same flow rate thermocapillarity is increased, the permanent waves take another form, presented in figure 11(*b*) for $Mn = 0.04$ ($R_c = 1.34$, $k_c = 2.35$ and $k_m = 1.67$). In this case, the thermocapillary force overcomes the stabilizing

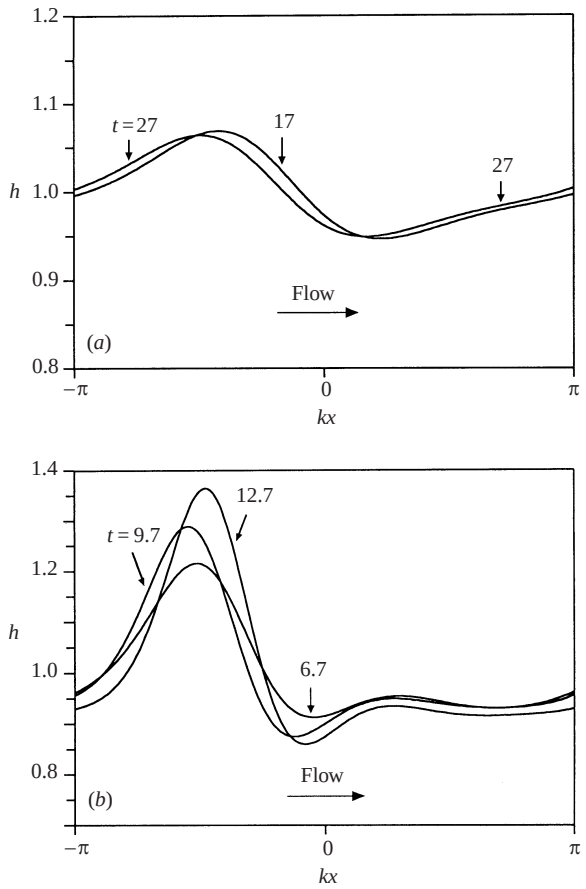

FIGURE 11. Free-surface configurations in the case of a linear increase in plate temperature for $R = 2.8$, $k = 1.3$ and: (*a*) $Mn = 0.02$ at $t = 17$ and $t = 27$ (final permanent waveform); (*b*) $Mn = 0.04$ at $t = 6.7$, $t = 9.7$ and $t = 12.7$.

effects of the hydrostatic pressure and mean surface tension. A significant steepening of the wave and a secondary wave structure are formed at the initial stage. Note that for $R = 2.8$ and $k = 1.3$ the growth rate of the corresponding isothermal layer monotonically decays until the surface is flattened. As seen in figure 11(*b*), thermocapillarity contributes little to the thinning of the film, so that dry spots will never be observed. As soon as a 'solitary' wave appears, the wave shape does not change significantly, but its amplitude varies until nonlinear saturation is attained.

In figure 12, the imposed wavenumber is decreased to $k = 0.9(\approx k_c/2)$, while R and Ma keep the same values as in figure 11(*a*) . Figure 12(*a*) shows how the initial finite-amplitude wave is dispersed into two waves of smaller amplitudes. In figure 12(*b*) are plotted three permanent wave shapes at different times. After nonlinear saturation, the only wave that could be recognized is of solitary type. Thus, by taking for R and k values above the neutral curve for $Mn = 0$ or slightly below it (see figure 3) and by imposing a weak non-uniform heating of the plate, the solution of the evolution equation (3.14) predicts nonlinear saturation, resulting in the formation of a finite-amplitude permanent wave.

The nonlinear interactions in non-uniformly heated falling films exhibit a tendency

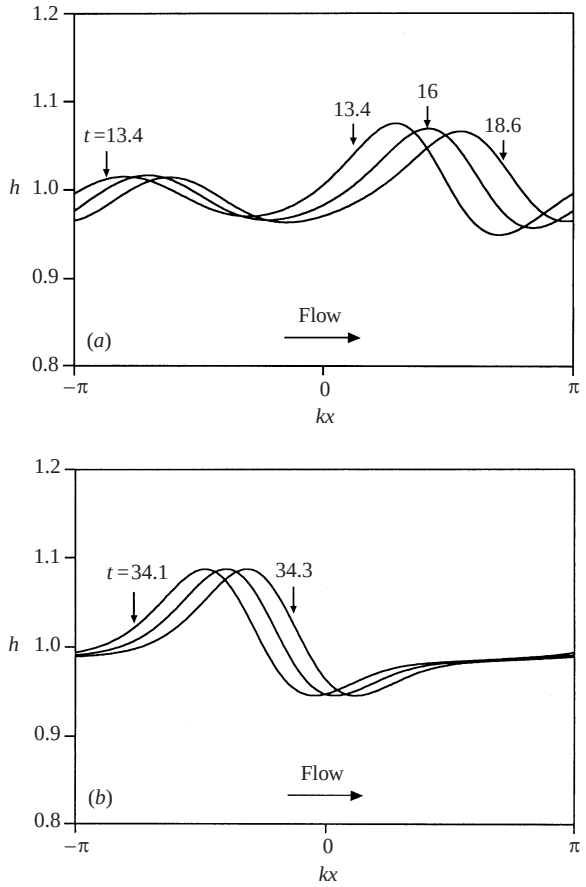

FIGURE 12. Free-surface configurations in the case of a linear increase in plate temperature for $R = 2.8$, $k = 0.9 \approx k_c/2$ and $Mn = 0.02$ at various instants of time: (*a*) from $t = 13.4$ to $t = 18.6$ in steps of 2.6; (*b*) final permanent waveforms for $34.1 \leqslant t \leqslant 34.3$ in steps of 0.1.

towards permanent two-dimensional waves for weak heating (at relatively small Marangoni number). When the Marangoni number is increased, nonlinear saturation has not been found because the thermocapillary force overcomes the stabilizing effects of the hydrostatic pressure and the mean surface tension and the film is destroyed.

5. Conclusions

The influence of a non-uniform heating of an inclined plate on the stability of a thin liquid film falling down it is investigated. A linear distribution of the plate temperature is assumed, so that a constant temperature gradient is acting. Both decreasing and increasing the plate temperature in the downstream direction are considered. The free surface is assumed adiabatic. The plate heating affects the film instability through the thermocapillary force acting along the free surface.

The goal of the present study is to quantify the effect of thermocapillarity on the non-linear instability of the falling film. For two-dimensional disturbances a long-wavelength evolution equation of the Benney-type is derived. It describes finite-amplitude instabilities due to viscosity, gravity, mean surface tension and thermocapillarity. The corresponding evolution equation differs from that obtained by Joo *et*

al. (1991) for a uniformly heated layer with a non-adiabatic free surface because of the presence of the thermocapillary effect. The Marangoni number defined by the longitudinal temperature gradient is positive (negative) when the plate temperature is increased (decreased) in the downstream direction.

The linear stability analysis of the equation yields the critical values of the Reynolds number and the dimensionless linearized phase speed for different values of the Marangoni number. The critical Reynolds number grows linearly with the absolute value of the Marangoni number if the plate temperature is decreased in the downstream direction ($Mn < 0$). In this case, the linear stability threshold increases with the Prandtl number. Increasing the plate temperature leads to a decrease of the critical Reynolds number. The reduction is important for large Prandtl numbers. So, decreasing the plate temperature in the downstream direction has a considerable stabilizing effect while the temperature increase plays a destabilizing role. The phase speed depends also on the direction of the heating. Being equal to the Reynolds number for isothermal films, it becomes larger (smaller) as the plate temperature is decreased (increased) in the flow direction.

The nonlinear stability analysis based on the numerical solution of the evolution equation confirms the results reported by Joo *et al.* (1991) for an isothermal film. We confirm, in particular, that finite-amplitude waves are stable solutions of the equation for initial wavenumbers smaller than the cut-off wavenumber. The permanent waves are nearly sinusoidal for initial wavenumbers close to the cut-off wavenumber and are of solitary type for much smaller values. It can be stated that the numerical results for the isothermal problem are in good agreement with calculations performed by other authors and experiments on thin-film flows.

A weakly nonlinear analysis is also performed to find a transition point k_s that separates the supercritical ($k > k_s$) from the subcritical ($k < k_s$) bifurcation. In the supercritical region, waves develop into permanent ones when they move downstream. But, their behaviour for k close to k_s cannot be adequately predicted by the weakly nonlinear theory. Numerical simulations are needed to determine the evolution of the permanent waves from the neutral stability curve when the wavenumber is decreased.

The general behaviour of non-uniformly heated films is similar to that of isothermal films, but the amplitude of the permanent waves is influenced by thermocapillarity. Depending on the direction of the imposed temperature gradient, the thermocapillary effect can be either stabilizing or destabilizing. If the plate temperature is decreased in the downstream direction, the thermocapillary force acts in the same direction and tends to flatten the free surface. As a consequence, the otherwise diverging disturbance in the isothermal film, converges either to the basic state of the flat surface or to a small-amplitude permanent wave.

When the plate temperature is increased in the downstream direction, the thermocapillary force acts in the opposite direction and thus promotes the growth rate of the wave amplitude with respect to the isothermal case. The shape of the permanent wave depends mainly on the flow rate measured by the Reynolds number, while its amplitude is influenced by thermocapillarity. A rapid amplitude growth is found for relatively large positive values of the Marangoni number, at least within the range of validity of the evolution equation derived in this work.

In summary, thermocapillarity influences the film shape but does not cause a significant local thinning of the film, leading to rupture. A supercritical bifurcation is predicted and it is shown that the preferred long-wave modes are of solitary type.

Obviously, non-isothermal film flows are mostly three-dimensional and such films need to be considered too. This will be the subject of a subsequent study. Here

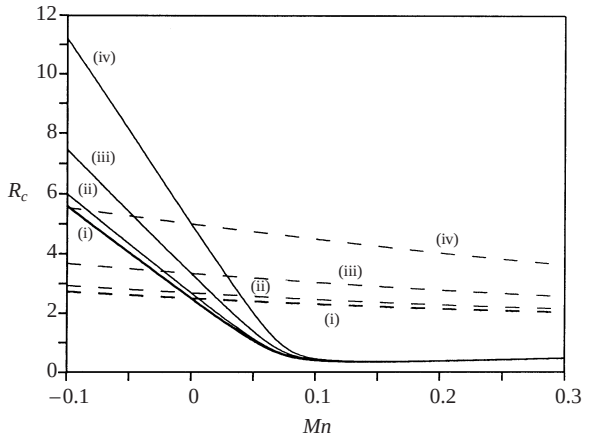

FIGURE 13. Critical Reynolds number versus Mn for $P = 1$ (dashed line) and $P = 10$ (solid line) and different angles: (i) $\varphi = 0$, (ii) $\varphi = \pi/12$, (iii) $\varphi = \pi/6$ and (iv) $\varphi = \pi/4$.

we present briefly the results of the linear stability analysis for three-dimensional disturbances. The corresponding evolution equation takes the following form:

$$h_t + (Rh - Mn)hh_x + \varepsilon\left[\tfrac{2}{15}Rh^5h_x(Rh - Mn)\right]_x + \varepsilon\nabla\cdot\left\{\left[\tfrac{1}{2}PMn\,h^4\left(\tfrac{5}{6}Rh - Mn\right) - \tfrac{1}{3}R\cot\beta h^3\right]\nabla h\right\} + \varepsilon\tfrac{1}{3}S\nabla\cdot[h^3\nabla\nabla^2 h] + O(\varepsilon^2) = 0. \tag{5.1}$$

Here ∇ is a two-dimensional gradient operator (∂_x, ∂_y), where y is the spanwise coordinate scaled by the characteristic length l. Imposing an infinitesimal harmonic disturbance with a wavenumber vector $\boldsymbol{k} = (k\cos\varphi, k\sin\varphi)$ in the (x, y)-plane, it is easy to calculate the linear growth rate

$$\omega_R = \varepsilon k^2\left[\tfrac{2}{15}R(R - Mn)\cos^2\varphi - \tfrac{1}{3}R\cot\beta - \tfrac{1}{3}k^2S + \tfrac{5}{12}RMnP - \tfrac{1}{2}PMn^2\right], \tag{5.2}$$

where φ is the angle between the plane in which the oblique wave propagates and the (x, z)-plane. In figure 13 the critical Reynolds number is plotted against the Marangoni number for three different oblique waves and the two-dimensional wave ($\varphi = 0$) presented in figure 2 (dashed lines for $P = 1$ and solid ones for $P = 10$). The linear stability analysis of isothermal as well as uniformly heated layers predicts that the two-dimensional waves are the most dangerous instability modes. According to the results of figure 13, this conclusion also holds for non-uniformly heated films with negative values of Mn when the plate temperature is decreased. For positive Mn, it remains true for $P = 1$, but not for $P = 10$, as there is no preferred two- or three-dimensional wave. The critical Marangoni number Mn^c, above which the initial instability will not be only two-dimensional, thus depends strongly on the Prandtl number. For $P = 10$, we find $Mn^c \approx 0.1$. A similar dependence of the preferred initial disturbance with respect to the Prandtl number was also noticed by Smith & Davis (1983) who studied the instability of non-uniformly heated horizontal layers.

In the present study, the Marangoni number is taken to be less than Mn^c and for this reason, the nonlinear two-dimensional analysis holds for the range of the non-dimensional parameters considered herein.

S. M. acknowledges the hospitality of the Department of Irreversible Thermodynamics at the University of Liege and the Federal Office for Scientific, Technical and Cultural Affairs, Belgium, for financial support. This work has also been supported by the European Community, Contract IC15-CT98-0908, C.C.E. ICOPAC Contract HRPN-CT-2000-00136 and by the Interuniversity Pole of Attraction (IUAP convention IV 06) initiated by the Belgian State, Science Policy Programming. We acknowledge the referees for their valuable suggestions for improving the text of the paper.

REFERENCES

Alekseenko, S. V., Nakoryakov, V. Ye. & Pokusaev, B. G. 1985 Wave formation on a vertical falling liquid film. *AIChE. J.* **31**, 1446–1460.

Alekseenko, S. V., Nakoryakov, V. Ye. & Pokusaev, B. G. 1994 *Wave Flow of Liquid Films.* Begell House.

Benjamin, T. B. 1957 Wave formation in a laminar flow down an inclined plane. *J. Fluid Mech.* **2**, 554–574.

Benney, D. J. 1966 Long waves on liquid films. *J. Maths. Phys.* **45**, 150–155.

Brauner, N. & Maron, D. M. 1982 Characteristics of inclined thin films waviness and the associated mass transfer. *Intl J. Heat Mass Transfer* **25**, 99–110.

Chang, H.-C. 1989 Onset of nonlinear waves of falling films. *Phys. Fluids* A **1**, 1314–1327.

Chang, H.-C. 1994 Wave evolution on a falling film. *Annu. Rev. Fluid Mech.* **26**, 103–136.

Chang, H.-C., Demekhin, E. A. & Kopelevich, D. I. 1993 Nonlinear evolution of waves on a vertically falling film. *J. Fluid Mech.* **250**, 433–480.

Davis, S. H. 1987 Thermocapillary instabilities. *Annu. Rev. Fluid Mech.* **19**, 403–435.

Demekhin, E. A. & Shkadov, V. Ya. 1985 Two-dimensional wave regimes of a thin liquid film. *Izv. Akad. Nauk. SSSR, Mekh. Zhid. i Gaza* **3**, 63–67.

Gjevik, B. 1970 Occurrence of finite-amplitude surface waves on falling liquid films. *Phys. Fluids* **13**, 1918–1925.

Goussis, D. A. & Kelly, R. E. 1990 On the thermocapillary instabilities in a liquid layer heated from below. *Intl J. Heat Mass Transfer* **33**, 2237–2245.

Goussis, D. A. & Kelly, R. E. 1991 Surface wave and thermocapillary instabilities in a liquid film flow. *J. Fluid Mech.* **223**, 25–45.

Joo, S. W. & Davis, S. H. 1992 Instabilities of three-dimensional viscous falling films. *J. Fluid Mech.* **242**, 529–547.

Joo, S. W., Davis, S. H. & Bankoff, S. G. 1991 Long-wave instabilities of heated falling films: two-dimensional theory of uniform layers. *J. Fluid Mech.* **230**, 117–146.

Joo, S. W., Davis, S. H. & Bankoff, S. G. 1996 A mechanism for rivulet formation in heated falling films. *J. Fluid Mech.* **321**, 279–298.

Kabov, O. A. 1998 Formation of regular structures in a falling liquid film upon local heating. *Thermophys. and Aeromech.* **5**, 547–551.

Kabov, O. A., Marchuk, I. V. & Chupin, V. M. 1996 Thermal imaging study of the liquid film flowing on vertical surface with local heat source. *Russ. J. Engng Thermophys.* **6**(2), 104–138.

Kabov, O. A., Marchuk, I. V., Muzykantov, A. V., Legros, J.-C., Istasse, E. & Dewandel, J. L. 1999 Regular structures in locally heated falling liquid films. In *Proc. 2nd Intl Symp. on Two-Phase Flow Modelling and Experimentation, Pisa* (ed. G. P. Celata, P. Di. Marco & R. K. Shah), vol. 5, pp. 1225–1233.

Kalitzova-Kurteva, P., Slavtchev, S. & Kurtev, I. 2000 Linear instability in liquid layers on an inclined, non-uniformly heated wall. *J. Theor. Appl. Mech.* **30**, No. 4, 12–23.

Kelly, R. E., Davis, S. H. & Goussis, D. A. 1986 On the instability of heated film flow with variable surface tension. *Heat Transfer 1986–Proc. 8th Intl Heat Transfer Conf.*, vol. 4, pp. 1937–1942. Hemisphere.

Krishnamoorthy, S., Ramaswamy, B. & Joo, S. W. 1995 Spontaneous rupture of thin liquid films due to thermocapillarity. A full-scale direct numerical simulation. *Phys. Fluids* **7**, 2291–2293.

Lin, S.-P. 1969 Finite amplitude stability of a parallel flow with a free surface. *J. Fluid Mech.* **36**, 113–126.

Lin, S.-P. 1974 Finite amplitude side-band stability of a viscous film. *J. Fluid Mech.* **63**, 417–429.

Lin, S.-P. 1975 Stability of liquid flow down a heated inclined plane. *Lett. Heat Mass Transfer* **2**, 361–370.

Liu, J., Paul, J. D. & Gollub, J. P. 1993 Measurements of the primary instabilities of film flows. *J. Fluid Mech.* **250**, 69–101.

Liu, J., Schneider, J. B. & Gollub, J. P. 1995 Three dimensional instabilities of film flows. *Phys. Fluids* **7**, 55–67.

López, P. G., Bankoff, S. G. & Miksis, M. J. 1996 Non-isothermal spreading of a thin liquid film on an inclined plane. *J. Fluid Mech.* **324**, 261–286.

Oron, A., Davis, S. H. & Bankoff, S. G. 1997 Long-scale evolution of thin liquid films. *Rev. Mod. Phys.* **69**, 931–980.

Prokopiou, Th., Cheng, M. & Chang, H.-C. 1991 Long waves on inclined films at high Reynolds number. *J. Fluid Mech.* **222**, 665–691.

Pumir, A., Manneville, P. & Pomeau, Y. 1983 On solitary waves running down an inclined plane. *J. Fluid Mech.* **135**, 27–50.

Ramaswamy, B., Chippada, S. & Joo, S. W. 1996 A full-scale numerical study of interfacial instabilities in thin-film flows. *J. Fluid Mech.* **325**, 163–194.

Salamon, T. S., Armstrong, R. C. & Brown, R. A. 1994 Traveling waves on vertical films: Numerical analysis using the finite element method. *Phys. Fluids* **6**, 2202–2220.

Scheid, B., Kabov, O., Minetti, C., Colinet, P. & Legros, J.-C. 2000 Measurement of free surface deformation by reflectance-Schlieren method. In *Proc. 3rd European Thermal-Science Conf., Heidelberg*, vol. 2, pp. 651–657.

Shkadov, V. Ya. 1967 Wave modes in the gravity flow of a thin layer of a viscous fluid. *Izv. Akad. Nauk. SSSR, Mekh. Zhid. i Gaza* **1**, 43–51.

Smith, M. K. & Davis, S. H. 1983 Instabilities of dynamic thermocapillary liquid layers. Part 2. Surface-wave instabilities. *J. Fluid Mech.* **132**, 145–162.

Sreenivasan, S. & Lin, S.-P. 1978 Surface tension driven instability of a liquid film flow down a heated incline. *Intl J. Heat Mass Transfer* **21**, 1517–1526.

Trifonov, Yu. Ya. & Tsvelodub, O. Yu. 1991 Nonlinear waves on the surface of a falling liquid film. Part 1. Waves of the first family and their stability. *J. Fluid Mech.* **229**, 531–554.

Yih, C.-S. 1963 Stability of liquid film down an inclined plane. *Phys. Fluids* **6**, 321–324.